

Condensed Matter Effects on Nuclear Fusion Rates in Laboratory and Astrophysical Environments

Y. E. Kim,¹ M. Rabinowitz,² and J.-H. Yoon¹

Received December 18, 1992

Previously overlooked condensed matter effects (CME) can significantly influence nuclear fusion rates in both laboratory and astrophysical environments. In dense plasmas, the ensemble of fusing particles has a significant exchange of kinetic and potential energies. Thus, there are diminished effective flux velocities resulting in a significant selective reduction of fusion rates. Our CME predictions are testable in laboratory experiments and have broad-ranging implications on the fusion rates for stellar media in general. By calculating reaction rates for $p(p, e^+ \nu_e)D$ and ${}^7\text{Be}(p, \gamma){}^8\text{B}$ in the sun, we show that CME help to solve the solar neutrino problem.

1. INTRODUCTION

This paper investigates condensed matter effects (CME) on nuclear fusion rates in laboratory and astrophysical environments. CME described in this paper are new and have not been included in previous calculations of nuclear fusion rates in laboratory beam experiments, magnetic and inertial fusion, and stellar fusion. Although CME is negligible for laboratory beam experiments at higher energies, it is shown that CME are not negligible for low-energy beam experiments and for stellar and solar environments. Our results imply that such calculations have to be redone with the inclusion of CME. The possibilities of testing CME using a low-energy beam in laboratory fusion experiments are presented.

In dense solar media, the flux of fusing nuclei is reduced predominantly due to elastic collisions in which the nuclei slow down as they approach the repulsive Coulomb barrier. For inelastic fusion collisions, the reduced velocity is properly included in the calculation for the tunneling probability,

¹Department of Physics, Purdue University, West Lafayette, Indiana 47907.

²Electric Power Research Institute, Palo Alto, California 94303.

and hence for the fusion cross section. However, we do not think the flux reduction has been properly accounted for even for inelastic collisions. Whether or not the flux is properly accounted for in inelastic collisions is not a crucial question in our paper, as the number of elastic collisions is some tens of orders of magnitude greater than the number of inelastic fusion collisions. Since the preponderance of the collisions do not involve tunneling, the flux reduction for most collisions has not been included in previous calculations. This effect on fusion rates is appreciable only at the high densities encountered in stellar media, and quickly diminishes at ordinary densities. The problem may be viewed with cautioned analogy to that of molecules in a gravitational potential where in the ideal case an altitude increase results only in a number density decrease with the maintenance of an isothermal Maxwellian distribution. However our problem is more complicated, as thermal equilibrium may not be restored locally when kinetic energy is converted to potential energy (cf. Section 5.2). In any case, the flux is reduced.

The fusion cross section σ and the flux velocity v are two main inputs for estimating the fusion rate $\langle\sigma v\rangle$. In our previous work (Kim *et al.*, 1992a, 1993), we have shown that the extrapolation method using a different but more realistic parametrization can give extrapolated values which are reduced by $\lesssim 30\%$ from the conventional estimate of $\sigma(v)$ involved in the fusion rate expression $\langle\sigma v\rangle$ for the ${}^7\text{Be}(p, \gamma){}^8\text{B}$ reaction. In this paper, we examine the validity of the use of the flux velocity v in the conventional fusion rate formula $\langle\sigma v\rangle$ for the case of a high-density medium. [The effective velocity we will introduce is not the customary average velocity defined as $\int |\mathbf{v}| f(\mathbf{v}) d^3v$, where $f(\mathbf{v})$ is given by equation (2.1) below.] As we will demonstrate, CME together with our corrections to fusion cross sections (Kim *et al.*, 1992a, 1993) can help to resolve the missing solar neutrino problem.

In Section 5, we point out an error in the conventional nuclear reaction rate equation for laboratory beam experiments, and present a corrected equation (5.2a). This correction is in addition to and independent of our condensed matter effects.

2. VELOCITY DISTRIBUTION IN DENSE PLASMA

For a (dilute) plasma in thermal equilibrium consisting of several species, the velocity distribution for the i th species is given by a Maxwell-Boltzmann (MB) distribution

$$f(\mathbf{v}_i) = \left(\frac{m_i}{2\pi kT}\right)^{3/2} \exp\left(\frac{-m_i v_i^2}{2kT}\right) \quad (2.1)$$

where T is the equilibrium temperature. Even though the processes are steady state, the fusing nuclei in the sun may not be in thermodynamic equilibrium, and it is possible to have a deviation from the MB distribution. However, it has been shown that deviations from the equilibrium MB distribution are small for the fusing nuclei from analysis involving solutions of the Boltzmann transport equation for the velocity distribution in the presence of Coulomb interactions (Bohm and Aller, 1947; MacDonald *et al.*, 1957). The same conclusion was also reached by Maxwell in 1866 (Maxwell, 1866).

When the plasma density is large as in the solar core, the potential energy w_i is no longer negligible and the kinetic energy is reduced from $m_i v_i^2/2$ to $m_i u_i^2/2$ ($m_i u_i^2 + w_i = m_i v_i^2/2$). Then the equilibrium MB distribution for u_i is given by (Kennard, 1938, pp. 77–90)

$$f(\mathbf{u}_i) = \left(\frac{m_i}{2\pi kT}\right)^{3/2} \exp\left[-\left(\frac{m_i u_i^2}{2} + w_i\right)/kT\right] \quad (2.2)$$

In this paper, both equations (2.1) and (2.2) will be used for the velocity distribution.

3. CONVENTIONAL FORMULAS FOR FUSION RATES

In the standard solar model (SSM) calculations of the solar neutrino flux, and stellar and laboratory fusion calculations, two of the basic inputs are the fusion reaction cross sections $\sigma(v)$ and the reaction rates. The fusion reaction rate (number of fusion events per unit volume per unit time) between two species of nuclei i and j is conventionally written as (Fowler *et al.*, 1967)

$$R_{\text{conv}} = \frac{n_i n_j}{1 + \delta_{ij}} \langle \sigma v \rangle_{\text{conv}} \quad (3.1)$$

where

$$\begin{aligned} \langle \sigma v \rangle_{\text{conv}} &= \int d^3 v_i \int d^3 v_j f(\mathbf{v}_i) f(\mathbf{v}_j) v \sigma(v) \\ &= \int d^3 v \int d^3 V f\left(\mathbf{V} + \frac{\mu}{m_i} \mathbf{v}\right) f\left(\mathbf{V} - \frac{\mu}{m_j} \mathbf{v}\right) v \sigma(v) \end{aligned} \quad (3.2)$$

with $\mathbf{v} = \mathbf{v}_i - \mathbf{v}_j$, $\mathbf{V} = (m_i \mathbf{v}_i + m_j \mathbf{v}_j)/(m_i + m_j)$, and the reduced mass $\mu = m_i m_j / (m_i + m_j)$. When the velocity distribution $f(\mathbf{v}_i)$ is the MB velocity distribution given by equation (2.1) with the normalization $\int f(\mathbf{v}_i) d^3 v = 1$, then

$$f(\mathbf{v}_i) f(\mathbf{v}_j) = f(\mathbf{V}) f(\mathbf{v}) \quad (3.3)$$

and hence equation (3.2) reduces to the following conventional form:

$$\begin{aligned} \langle \sigma v \rangle_{\text{conv}} &= \int \sigma(v) v f(v) d^3v \\ &= \left(\frac{8}{\pi\mu} \right)^{1/2} \frac{1}{(kT)^{3/2}} \int_0^\infty \sigma(E) E \exp\left(-\frac{E}{kT}\right) dE \end{aligned} \quad (3.4)$$

with kinetic energy $E = \mu v^2/2$, in the center-of-mass (CM) frame. The low-energy cross section $\sigma(E)$ in equation (3.4) cannot be measured directly in the laboratory, due to small reaction rates at low energies ($\sim \text{keV}$) corresponding to the solar core temperature ($\sim 1.4 \times 10^7 \text{ K}$). Therefore theoretical estimates and/or extrapolated values for $\sigma(E)$ are used in equation (3.4) to evaluate $\langle \sigma v \rangle_{\text{conv}}$ at low energies. It is important to emphasize that v in $\langle \sigma v \rangle_{\text{conv}}$ is related to the (incident) flux and is to be distinguished from v appearing in $\sigma(v)$ and $f(v)$ in equation (3.4), as discussed in Section 4.

Conventional low-energy ($< 20 \text{ keV}$) $\sigma(E)$ are calculated either from nuclear theory or by extrapolating the experimental values of $\sigma(E)$ at higher energies using the parametrization (Fowler *et al.*, 1967)

$$\sigma(E) = [S(E)/E] \exp(-E^{1/2}/E_G^{1/2}) \quad (3.5)$$

where $E_G = (2\pi\alpha Z_i Z_j)^2 \mu c^2/2$. The ‘‘Gamow’’ factor, $\exp(-E^{1/2}/E_G^{1/2})$ in equation (3.5) represents the transmission coefficient for bringing two charged particles (Z_i and Z_j) to zero separation distance, which is unphysical and unrealistic, since it implies that the Coulomb barrier $Z_i Z_j e^2/r$ also exists inside the nuclear surface of radius r_N (Kim *et al.*, 1992a, 1993).

In laboratory beam experiments, the fusion reaction rate (number of fusion events per unit area per unit time) is written as

$$R_{\text{conv}}^{\text{beam}}(E_i) = n_t \phi_i \int \sigma dx = n_t n_i v_i \int_{E_i - \Delta E}^{E_i} \frac{\sigma(E)}{|dE'/dx|} dE' \quad (3.6)$$

where n_t is the target atom number density, $\phi_i = n_i v_i$ is the incident beam flux (number of incident particles per unit time and per unit area), dE/dx is the stopping power for the beam projectile by the target atom (Anderson and Ziegler, 1977; Kim *et al.*, 1991), which includes the effect of the energy loss due to other inelastic scatterings in addition to the energy-conserving elastic scattering characterized by the elastic cross section σ_e , and $E_i = m_i v_i^2/2$ is the incident kinetic energy. Both E_i and E' are in the laboratory (LAB) frame, while E is in the CM frame.

4. CONDENSED MATTER ENERGY EXCHANGE EFFECT (CMEE)

In this section, we show that the incident flux characterized by v or v_i in equations (3.4) and (3.6) needs to be modified to an average velocity $\bar{v} \leq v$ at low energies in condensed matter environments, and that CME help to solve the solar neutrino problem (Rowley *et al.*, 1987; Davis, 1988; Bahcall, 1969; Bahcall and Ulrich, 1988; Turck-Chièze *et al.*, 1988; Bahcall and Pinsonneault, 1992; Hirata *et al.*, 1989, 1990; Anselmann *et al.*, 1992; Kuo and Pantaleone, 1989). This has been neglected in conventional fusion rate calculations. If the initial velocity $v = v_i$ is specified as that which satisfies the Maxwell-Boltzmann velocity distribution or as that of the incident projectile, the particle with initial incident velocity v_i will undergo many (elastic) collisions (characterized by an elastic cross section σ_e) before it fuses with the target nucleus (characterized by a fusion cross section, $\sigma_f \ll \sigma_e$).

The elastic cross section σ_e can be estimated within an order of magnitude using a screened Coulomb potential given by

$$V_{sc}(r) = \frac{Z_i Z_j e^2}{r} e^{-r/a} \tag{4.1}$$

The total elastic cross section $\sigma_{sc}(E)$ for $V_{sc}(r)$ in the Born approximation (Schiff, 1968, p. 325) can be written as

$$\sigma_{sc}(E) = \frac{16\pi\mu^2(Z_i Z_j)^2 e^4 a^4}{\hbar^4(4k^2 a^2 + 1)} \tag{4.2}$$

where $\hbar^2 k^2 / 2\mu = E$ and a is a screening radius. For energies considered in this paper, $4k^2 a^2 \gg 1$, and hence equation (4.2) can be written accurately as

$$\sigma_{sc}(E) = 4\pi a^2 \frac{e^4 (Z_i Z_j)^2}{\hbar^2 v^2} \tag{4.3}$$

where $v = \hbar k / \mu$.

Since the values of $V_{sc}(r)$ at interatomic distance $a \approx 0.2\text{--}1.0 \text{ \AA}$ are of the order of 10 eV and are much smaller than $E \approx 1\text{--}10 \text{ keV}$, we approximate $V_{sc}(r)$ by a “shifted” screened Coulomb potential $V_s(r)$ with an interior square-well nuclear potential for the purpose of obtaining quantitative estimates of CMEE:

$$V_s(r) = \begin{cases} -V_0, & r < r_N \\ Z_i Z_j e^2 \left(\frac{1}{r} - \frac{1}{r_s} \right), & r_s > r \geq r_N \\ 0, & r_e > r \geq r_s \end{cases} \tag{4.4}$$

$V_s(r)$ is shown schematically in Fig. 1.

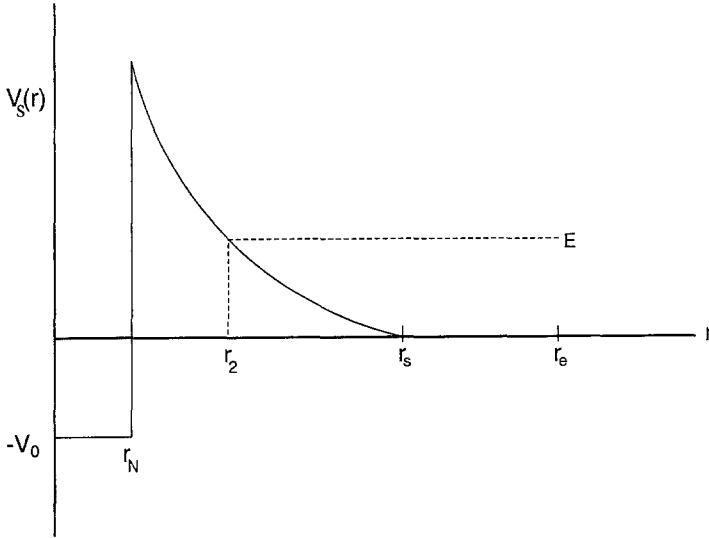


Fig. 1. Schematic plot of the "shifted" screened Coulomb potential, equation (4.4), used in this paper.

4.1. Single-Species Case

For a number density of condensed (target) matter n and elastic cross section σ_e , the mean free path can be defined as

$$\lambda_e = \frac{1}{n\sigma_e} = r_e - r_2 \quad (4.5)$$

and for σ_f ,

$$\lambda_f = \frac{1}{n\sigma_f} + r_2 = \frac{\lambda_e \sigma_e}{\sigma_f} + r_2 \quad (4.6)$$

where r_2 is chosen as the classical distance of closest approach (turning point) for a given barrier. The average interatomic distance is $\sim 2r_e$ in condensed matter. We note that $(r_e - r_s) \gg \lambda_d$ for nuclei moving with kinetic energy, $E > 10^3$ eV, where $\lambda_d = h/(2mE)^{1/2}$ is the de Broglie wavelength, permitting the standard calculation of the tunneling coefficient. Then the effective flux velocity (\propto effective flux) can be written as

$$\begin{aligned} \langle v \rangle &= \frac{\lambda_f}{(t_i + t_0)(\sigma_e/\sigma_f) + t_B + t_N} \\ &= \frac{(r_e - r_2)(\sigma_e/\sigma_f) + r_2}{(t_i + t_0)(\sigma_e/\sigma_f) + t_B + t_N} \end{aligned} \quad (4.7)$$

where t_i , t_0 , t_B , and t_N are the times for the incident particles to traverse distances $(r_e - r_s)$, $(r_s - r_2)$, $(r_2 - r_N)$, and r_N , respectively. Using equations (4.2) or (4.3), it can be shown that $\sigma_{sc} \gg \sigma_f$. Since σ_e is of order of σ_{sc} , we have $\sigma_e \gg \sigma_f$. For the case of $\sigma_e \gg \sigma_f$, $\langle v \rangle$ given by equation (4.7) reduces to

$$\langle v \rangle \approx \bar{v} = \frac{r_e - r_2}{t_i + t_0} = \frac{(r_e - r_s) + (r_s - r_2)}{t_i + t_0} \tag{4.8}$$

We will show below that $\bar{v} \leq v$, where v is given by

$$v = v_i = \frac{r_e - r_s}{t_i} \tag{4.9}$$

We note that our effective velocity $\langle v \rangle$, equation (4.7) or equation (4.8), is not the customary average velocity defined as $\int |\mathbf{v}| f(\mathbf{v}) d^3v$.

The traversal time $t(j) = t_0$ of the incident particle i in equation (4.8) in the presence of the barrier due to the target species j can be estimated in the WKB approximation for the case of $V_s(r)$, equation (4.4), with $E < B = V_s(r_N)$ as

$$\begin{aligned} t(j) &= \int_{r_2(j)}^{r_s(j)} \left[\frac{2}{\mu_{ij}} |E - V_s(r)| \right]^{-1/2} dr \\ &= r_s(j) \left[\frac{\mu_{ij}}{2E'(j)} \right]^{1/2} \left[\frac{E(j)}{E'(j)} \right]^{1/2} L_j(E) \end{aligned} \tag{4.10}$$

where $\mu_{ij} = m_i m_j / (m_i + m_j)$, $E(j) = E$, and

$$L_j(E) = 1 + \left[\frac{E_s(j)}{E'(j)} \right]^{1/2} \left[\frac{E_s(j)}{E(j)} \right]^{1/2} \ln \left\{ \left[\frac{E'(j)}{E_s(j)} \right]^{1/2} + \left[\frac{E(j)}{E_s(j)} \right]^{1/2} \right\} \tag{4.10a}$$

with

$$E'(j) = E(j) + E_s(j) = Z_i Z_j e^2 / r_2(j) \tag{4.10b}$$

and

$$E_s(j) = Z_i Z_j e^2 / r_s(j) \tag{4.10c}$$

Using equation (4.10) in equation (4.8), we obtain for the flux velocity reduction factor $F^{(ij)}(E) = \bar{v}/v$

$$F^{(ij)}(E) = \frac{1 + E_s(j) E'(j) / (E_e E)}{L_j(E) + E_s(j) E'(j) / (E_e E)} \tag{4.11}$$

where $E = E(j)$, and E_e is defined as

$$E_e = \frac{Z_i Z_j e^2}{\chi} \tag{4.12}$$

with

$$\chi = r_{es} = r_e - r_s = r_e(j) - r_s(j) \tag{4.13}$$

We note that $\lim_{E \rightarrow 0} F^{(ij)}(E) = 1$, $\lim_{E \rightarrow B} F^{(ij)}(E) \approx 1$, and $F^{(ij)}(E) \leq 1$.

4.2. Two-Species Case

For the case of two species in the target (one species with a number density n_j participating in fusion reaction with the incident particle i and other nonparticipating species with a number density n_k), equation (4.8) for \bar{v} can be generalized as

$$\begin{aligned} \bar{v} &= \frac{p_j \sigma_e(j) r_{s2}(j) + p_k \sigma_e(k) r_{s2}(k) + (p_j \sigma_e(j) + p_k \sigma_e(k)) r_{es}}{p_j \sigma_e(j) t(j) + p_k \sigma_e(k) t(k) + (p_j \sigma_e(j) + p_k \sigma_e(k)) t_i} \\ &= \frac{r_{s2}(j) + \delta \sigma_{kj} r_{s2}(k) + (1 + \delta \sigma_{kj}) r_{es}}{t(j) + \delta \sigma_{kj} t(k) + (1 + \delta \sigma_{kj}) t_i} \end{aligned} \tag{4.14}$$

where $\delta = p_k/p_j$, $\sigma_{kj} = \sigma_e(k)/\sigma_e(j)$, $r_{s2}(j) = r_s(j) - r_2(j)$, $r_{es} = r_e(j) - r_s(j)$, and we assumed $r_e(k) - r_s(k) = r_{es}$. Here p_j and p_k are collision probabilities given by $p_j = n_{ij}/(n_{ij} + n_{ik})$ and $p_k = n_{ik}/(n_{ij} + n_{ik})$, respectively, with $n_{ij} = n_i n_j / (1 + \delta_{ij})$ for plasma fusion or with $n_{ij} = n_i n_j$ for laboratory beam fusion. If we assume $\sigma_e \propto \sigma_{sc}$, the ratio $\sigma_{kj} = \sigma_e(k)/\sigma_e(j)$ can be estimated using equation (4.3) as

$$\sigma_{kj} = \frac{\sigma_e(k)}{\sigma_e(j)} = \left(\frac{a_k Z_k}{a_j Z_j} \right)^2 \beta_{kj} \tag{4.15}$$

with $\beta_{kj} = E(k)/E(j) = \mu_{ik}/\mu_{ij}$.

Using equation (4.10) in equation (4.14), we obtain for the flux velocity reduction factor $F(E) = \bar{v}/v$

$$\begin{aligned} F_{\chi}^{(i,j,k)}(E) &= \left[1 + \delta \sigma_{kj} \left(\frac{1}{\gamma_{kj}} \right) \frac{E'(j)}{E'(k)} + (1 + \delta \sigma_{kj}) \frac{E_s(j) E'(j)}{E_e E} \right] \\ &\times \left\{ L_j(E) + \delta \sigma_{kj} \left(\frac{1}{\gamma_{kj}} \right) \frac{E'(j)}{E'(k)} L_k(E) \right. \\ &\left. + (1 + \delta \sigma_{kj}) \frac{E_s(j) E'(j)}{E_e E} \right\}^{-1} \end{aligned} \tag{4.16}$$

where $L_j(E)$, $E'(j)$, and E_e are given by equations (4.10a), (4.10b), and (4.12), respectively, and

$$E'(k) = E(k) + E_s(k) = E + \gamma_{kj} E_s(j) \tag{4.16a}$$

with $\gamma_{kj} = E_s(k)/E_s(j)$. It can be easily shown that $\lim_{E \rightarrow B} F_\chi(E) \approx 1$, $\lim_{E \rightarrow 0} F_\chi(E) = 1$, and $F_\chi(E) \leq 1$. Equation (4.16) reduces to equation (4.11) in the limit of $Z_k \rightarrow 0$ corresponding to the case of a single species target. The $\lim_{E \rightarrow 0} F_\chi = 1$ is an artifact of our simplified shielding, which permits $r_e - r_s \neq 0$.

For the case of $r_{es} = 0$ and hence $t_i = 0$, equation (4.16) reduces to

$$F_0^{(i,j,k)}(E) = \left[1 + \delta\sigma_{kj} \left(\frac{1}{\gamma_{kj}} \right) \frac{E'(j)}{E'(k)} \right] \times \left[L_j(E) + \delta\sigma_{kj} \left(\frac{1}{\gamma_{kj}} \right) \left(\frac{E'(j)}{E'(k)} \right) L_k(E) \right]^{-1} \tag{4.17}$$

We note that $\lim_{E \rightarrow B} F_0(E) \approx 1$, $\lim_{E \rightarrow 0} F_0(E) = 1/2$, and $F_0(E) \leq 1$. In the following, \bar{v} will be referred to as the flux velocity to distinguish it from v appearing in $\sigma(v)$ and $f(v)$ in equation (3.4).

5. REVISED FORMULAS FOR FUSION RATES

In this section, we show that the velocity \bar{v} given by equation (4.8) or (4.14) is the appropriate value to be used in equation (3.4) or equation (3.6) rather than $v (=v_i)$ given by equation (4.9) which has been used in the conventional equations (3.4) and (3.6). We also present new revised fusion rate formulas applicable to laboratory and astrophysical environments.

5.1. Laboratory Beam Experiments

If a projectile particle i moves through a condensed matter target, then the probability of a fusion reaction per unit path length of the projectile is $P_x = n_t \sigma$. Because of the elastic scattering processes described in the previous section, the projectile path length per unit time in the target is \bar{v} , and not v . Hence, the probability of fusion for the projectile path length per unit time is $P' = \bar{v} n_t \sigma$. However, in addition to the reduced velocity $\bar{v} < v$ due to the (energy-conserving) elastic scattering in the CM frame described in the previous section, there is further slowing down of the projectile in the target material due to the stopping power by target atoms [energy loss of the projectile by elastic scattering in the LAB frame (energy transfer) and

also by inelastic scattering from target atoms]. Therefore, the effective fusion length per unit time is reduced to

$$P = \int P' dx = \eta_t \int \sigma \bar{v} dx \quad (5.1)$$

and the new revised fusion rate in terms of the incident flux $\phi_i = n_i v_i$ is given by

$$\begin{aligned} R_{\text{new}}^{\text{beam}}(E_i) &= n_i P = n_i n_i v_i \int \sigma(v) (\bar{v}/v) (v/v_i) dx \\ &= n_i \phi_i \int_{E_i - \Delta E}^{E_i} \frac{\sigma(E) (\bar{v}/v) (v/v_i)}{|dE'/dx|} dE' \\ &= n_i \phi_i \int_{E_i - \Delta E}^{E_i} \frac{\sigma(E) F_x(E) (E'/E_i)^{1/2}}{|dE'/dx|} dE' \end{aligned} \quad (5.2)$$

where E and E' are kinetic energies in the CM and LAB frames, respectively, i.e., $E = \mu v^2/2$, $E' = m_i v'^2/2$, and $E_i = m_i v_i^2/2$. The $\sigma(v)$ [or $\sigma(E)$] in equation (5.2) is still to be evaluated with v instead of \bar{v} , since the cross section is defined in terms of the assumed incident flux v and is extracted either from experiments or from theoretical calculations using v instead of \bar{v} .

5.1.1. Erroneous Interpretation of Laboratory Beam Experiments

For laboratory beam experiments, the conventional fusion rate expression for $R_{\text{conv}}^{\text{beam}}(E_i)$ given by equation (3.6) has been commonly used by experimentalists to extract $\sigma(E)$ from the values of $R_{\text{conv}}^{\text{beam}}(E_i)$ obtained from the experimental measurement. However, even without the inclusion of the new condensed matter effects, *the conventional fusion rate equation* $R_{\text{conv}}^{\text{beam}}(E)$ given by equation (3.6) is *incorrect* and needs to be modified to

$$\begin{aligned} \tilde{R}_{\text{conv}}^{\text{beam}}(E_i) &= n_i n_i v_i \int_{E_i - \Delta E}^{E_i} \frac{\sigma(E) (v/v_i)}{|dE'/dx|} dE' \\ &= n_i n_i v_i \int_{E_i - \Delta E}^{E_i} \frac{\sigma(E) (E'/E_i)^{1/2}}{|dE'/dx|} dE' \end{aligned} \quad (5.2a)$$

5.1.2. Fusion Cross-Section Parametrization

We now parametrize $\sigma(E)$ as

$$\sigma(E) = \frac{S_s(E)}{E} T_s(E) \quad (5.3)$$

where $T_s(E)$ is the transmission coefficient computed for $V_s(r)$ given by equation (4.4) (Kim *et al.*, 1992a, 1993). We note that $T_s(E)$ calculated from $V_s(r)$ is more realistic and physical than $\exp(-E_G^{1/2}/E^{1/2})$ used in equation (3.5).

We introduce another parametrization of $\sigma(E)$ with a potential $V_{ns}(r)$ without the electron screening consisting of an interior square-well nuclear potential and an exterior Coulomb repulsive potential,

$$V_{ns}(r) = \begin{cases} -V_0, & r < R = r_N \\ \frac{Z_i Z_j e^2}{r}, & r \geq R = r_N \end{cases} \quad (5.4)$$

and write $\sigma(E)$ as

$$\sigma(E) = \frac{\tilde{S}(E)}{E} T_{ns}(E) \quad (5.5)$$

where $T_{ns}(E)$ is the transmission coefficient with $V_{ns}(r)$, and is nearly the same as $T_s(E)$ for $E > Z_i Z_j e^2 / r_s$ (~ 100 eV). One practical advantage of using $V_{ns}(r)$ is that $T_{ns}(E)$ can be expressed in terms of known Coulomb wave functions (Blatt and Weisskopf, 1954; Kim *et al.*, 1992a, 1993). For the S -wave scattering cross section, we have

$$T_{ns}(E) = \frac{4s_0 KR}{\Delta_0^2 + (s_0 + KR)^2} \quad (5.6)$$

where

$$s_0 = R[(\tilde{G}_0 \tilde{F}'_0 - \tilde{F}_0 \tilde{G}'_0)/(\tilde{G}_0^2 + \tilde{F}_0^2)]_{r=R} \quad (5.6a)$$

$$\Delta_0 = R[(\tilde{G}_0 \tilde{G}'_0 + \tilde{F}_0 \tilde{F}'_0)/(\tilde{G}_0^2 + \tilde{F}_0^2)]_{r=R} \quad (5.6b)$$

and $\hbar^2 K^2 / 2\mu = V_0 + E$ with $E = \hbar^2 k^2 / 2\mu$. Here \tilde{F}'_0 and \tilde{G}'_0 are derivatives of \tilde{F}_0 and \tilde{G}_0 with respect to r , and \tilde{F}_0 and \tilde{G}_0 are the regular and irregular Coulomb wave functions normalized asymptotically ($r \rightarrow \infty$) as $\tilde{F}_0(r) \approx \sin[kr - \eta \ln(2kr) + \sigma_0]$ and $\tilde{G}_0(r) \approx \cos[kr - \eta \ln(2kr) + \sigma_0]$. The σ_0 is the S -wave Coulomb phase shift, $\sigma_0 = \arg \Gamma(1 + i\eta)$, with the Sommerfeld parameter $\eta = Z_i Z_j e^2 / \hbar v$. The incoming flux is normalized to unity, $\tilde{G}_0^2 + \tilde{F}_0^2 = 1$, for $r \rightarrow \infty$.

5.2. Astrophysical Environments

For dense astrophysical or laboratory plasmas, when a projectile particle i moves through the plasma with velocity $u = \bar{v}$, the probability of a fusion reaction per unit path length of the projectile is given by $P_x = n_j \sigma$,

where n_j is the number of target nuclei per unit volume of the plasma. As in the previous case of laboratory beam experiments, the projectile traversal distance per unit time is u (not v). Then the fusion reaction probability for the projectile path length per unit time is $P = uP_x = un_j\sigma(u)$. If the plasma through which the projectile moves is isotropic, the probability of a fusion reaction is independent of the direction in which the projectile is moving. The rate at which n_i projectiles per unit volume, each moving with a speed $u(v)$ but in random directions, will react is then $R(u) = n_i u P_x = (n_i u)(n_j \sigma(u))$.

Using equation (2.2), the velocity distribution for u is given by

$$f(u) = \left(\frac{\mu}{2\pi kT}\right)^{3/2} \exp\left[\frac{-(\mu u^2/2 + W)}{kT}\right] \quad (5.7)$$

where $W \equiv \mu v^2/2 - \mu u^2/2$. Since $f(u)$ does not conserve the particle number due to $\int f(u) d^3u \neq 1$, we replace $f(u)$ by $\tilde{f}(u)$,

$$\begin{aligned} \tilde{f}(u) &= f(u) \left(\frac{d^3v}{d^3u}\right) \\ &= \left(\frac{\mu}{2\pi kT}\right)^{3/2} \exp\left(\frac{-\mu v^2}{kT}\right) \left(\frac{d^3v}{d^3u}\right) \end{aligned} \quad (5.8)$$

with the normalization $\int \tilde{f}(u) d^3u = 1$.

We note that $\langle \mu u^2/2 \rangle \equiv 3k\tau/2$ is given by

$$\begin{aligned} \frac{3k\tau}{2} &\equiv \left\langle \frac{\mu u^2}{2} \right\rangle = \int \left(\frac{\mu u^2}{2}\right) \tilde{f}(u) d^3u \\ &= \left(\frac{1}{\pi}\right)^{1/2} \frac{2}{(kT)^{3/2}} \int_0^\infty F_0^2 E^{3/2} e^{-E/kT} dE \end{aligned} \quad (5.9)$$

Since

$$\langle \mu v^2/2 \rangle = \int (\mu v^2/2) \tilde{f}(u) d^3u = \int (\mu v^2/2) f(v) d^3v = 3kT/2$$

we have

$$\langle W \rangle = \langle \mu v^2/2 \rangle - \langle \mu u^2/2 \rangle = 3kT/2 - 3k\tau/2$$

If a projectile velocity distribution $\tilde{f}(u)$ is given, then the new fusion rate is given by

$$R_{\text{new}} = \frac{n_i n_j}{1 + \delta_{ij}} \langle \sigma v \rangle_{\text{new}} \quad (5.10)$$

where

$$\begin{aligned} \langle \sigma v \rangle_{\text{new}} &= \int \sigma(u) u \tilde{f}(u) d^3u \\ &= \int \sigma(u) u f(v) d^3v \\ &= \left(\frac{8}{\pi\mu}\right)^{1/2} \frac{1}{(kT)^{3/2}} \int_0^\infty \sigma(\bar{E}) F_0(E) E \exp\left(-\frac{E}{kT}\right) dE \quad (5.11) \end{aligned}$$

where $\bar{E} = EF_0^2(E)$. Justification for using $F_0(E)$ [equation (4.17)] in equation (5.11) rather than $F_x(E)$ [equation (4.16)] is given in Section 6.2. We note that $\langle \sigma v \rangle_{\text{new}} \leq \langle \sigma v \rangle_{\text{conv}}$.

In an almost equivalent option, we can use

$$\tilde{f}(u) = (\mu/2\pi kT)^{3/2} \exp(-\mu u^2/2kT)$$

as the velocity distribution for u instead of $\tilde{f}(u)$, equation (5.8), and interpret $\exp[-W(u)/kT]$ in equation (5.7) as a pair correlation function which reduces the probability factor (or effectively, number densities) $n_i n_j$ to $n_i n_j \exp[-W(u)/kT]$ in the fusion rate, $R_{\text{new}} = [n_i n_j / (1 + \delta_{ij})] \langle \sigma v \rangle_{\text{new}}$. The above interpretation yields a new revised fusion rate $\langle \sigma v \rangle'_{\text{new}}$ given by

$$\langle \sigma v \rangle'_{\text{new}} = \int e^{-W(u)/kT} \sigma(u) u \tilde{f}(u) d^3u = \int \sigma(u) u f(v) d^3u \quad (5.12)$$

where $f(v) = (\mu/2\pi kT)^{3/2} \exp(-\mu v^2/kT)$. The results calculated from equation (5.12) agree with those from equation (5.11) within 2% and hence only the results of equation (5.11) will be presented in this paper.

Two additional possibilities are to replace $\sigma(u)$ by $\sigma(v)$ or $\sigma(u_{\text{rms}})$ in the integrals of equations (5.11) and (5.12), where u_{rms} is the root mean square flux velocity. We favor $\sigma(u)$ in equations (5.11) and (5.12), since, as we explained in the beginning of Section 5.2, the fusion reaction probability is proportional to $un_j \sigma(u)$ involving u rather than v or u_{rms} .

6. APPLICATIONS AND RESULTS

We now apply our new CME formulation [equations (4.11), (4.16), (4.17), (5.2), and (5.11)] of nuclear fusion rates to specific cases.

6.1. ${}^7\text{Be}(p, \gamma){}^8\text{B}$ Laboratory Beam Experiment

For the laboratory beam experiment ${}^7\text{Be}(p, \gamma){}^8\text{B}$ with ${}^7\text{Be}^{16}\text{O}$ target (Filippone *et al.*, 1983; Kavanagh *et al.*, 1969), $\delta = 1$, and the indices i, j ,

and k in equation (4.16) are identified as p , ${}^7\text{Be}$, and ${}^{16}\text{O}$, respectively. Using $\rho({}^7\text{Be}{}^{16}\text{O}) = 2.77 \text{ g/cm}^3$, we obtain the interatomic distance between ${}^7\text{Be}$ and ${}^{16}\text{O}$ as 2.40 \AA . We choose $r_s(j) = 1.05 \text{ \AA}$ and $r_s(k) = 0.60 \text{ \AA}$ to be the neutral atom sizes of Be and O, respectively. Then from equation (4.10c), $E_s(j) = 0.055 \text{ keV}$, $E_s(k) = 0.192 \text{ keV}$, and $\gamma_{kj} = E_s(k)/E_s(j) \approx 3.50$. Since $r_{es} = \{2.40 \text{ \AA} - [r_s(j) + r_s(k)]\}/2 = 0.375 \text{ \AA}$, $E_e = 0.154 \text{ keV}$ from equation (4.12). For $Z_i = 1$, $Z_j = 4$, $Z_k = 8$, $a_j = a_0(Z_j)^{-1/3}$ (a_0 is the Bohr radius), and $a_k = a_0(Z_k)^{-1/3}$ (Bohr, 1948), we obtain $\sigma_{kj} = 2.71$ from equation (4.15). Also $\beta_{kj} \cong (16/17)/(7/8) \approx 1.076$.

Using the above numerical values for the case of ${}^7\text{Be}(p, \gamma){}^8\text{B}$ with a ${}^7\text{Be}{}^{16}\text{O}$ target in the laboratory, equation (4.16) can be written as (E in keV)

$$F_{\chi}^{(1,7,16)}(E) = \frac{1 + 0.78E'(j)/E'(k) + 1.325E'(j)/E}{L_j(E) + 0.78[E'(j)/E'(k)]L_k(E) + 1.325E'(j)/E} \quad (6.1)$$

where $E'(j) = E + 0.055 \text{ keV}$ from equation (4.10b) and $E'(k) = E + 0.192 \text{ keV}$ from equation (4.16a). From equation (4.10a), $L_j(E) = 1 + [\ln(W'_j + W_j)]/W'_j W_j$ with $W'_j = [(E + 0.055)/0.055]^{1/2}$ and $W_j = (E/0.055)^{1/2}$, and $L_k(E) = 1 + [\ln(W'_k + W_k)]/W'_k W_k$ with $W'_k = [(E + 0.192)/0.192]^{1/2}$ and $W_k = (E/0.192)^{1/2}$. Numerical values of $F_{\chi}^{(1,7,16)}(E)$, equation (6.1), are plotted as a function of E in Fig. 2 (solid curve).

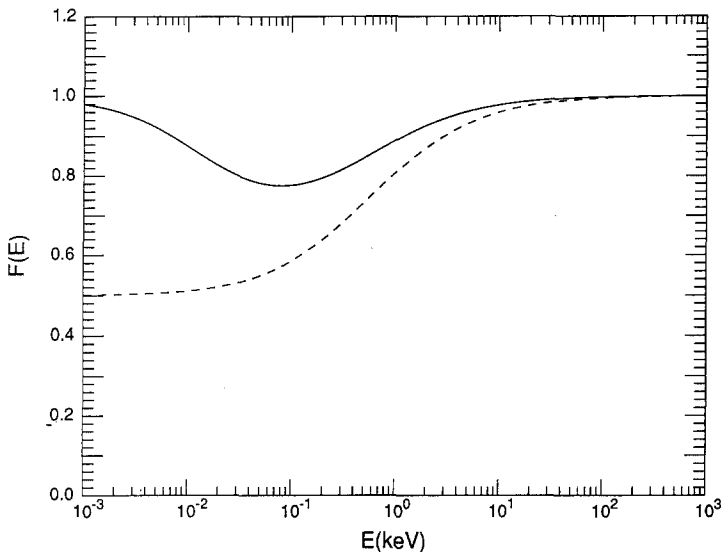


Fig. 2. Flux velocity reduction factors $F(E)$ for ${}^7\text{Be}(p, \gamma){}^8\text{B}$ with a ${}^7\text{Be}{}^{16}\text{O}$ target in a laboratory environment [equation (6.1), solid line] and for ${}^7\text{Be}(p, \gamma){}^8\text{B}$ in the sun [equation (6.3), dashed line], as a function of $E = \mu v^2/2$.

Since the experimental data (Filippone *et al.*, 1983; Kavanagh *et al.*, 1969) for ${}^7\text{Be}(p, \gamma){}^8\text{B}$ are for higher energies ($E \gtrsim 100$ keV) and $F_{\chi}^{(1,7,16)}(E) \approx 1$ for $E \gtrsim 100$ keV, the revised fusion rate $R_{\text{new}}^{\text{beam}}$, equation (5.2), is expected to be nearly the same as that obtained from $\tilde{R}_{\text{conv}}^{\text{beam}}$, equation (5.2a), for $E \gtrsim 100$ keV. Therefore, extrapolation of $\sigma(E)$ to lower energies $E < 100$ keV can be made using equation (3.5), (5.3), or (5.5) without CMEE and $F_{\chi}^{(1,7,16)}(E)$. However, the use of the incorrect form $R_{\text{conv}}^{\text{beam}}$, equation (3.6), in extracting $\sigma(E)$ from measured fusion rates may yield underestimates of $\sigma(E)$. It will be difficult to test equation (5.2) with the ${}^7\text{Be}(p, \gamma){}^8\text{B}$ reaction due to low counting rates at low energies, but the measurement of the fusion rates for other reactions, such as $\text{D}(\text{D}, p)\text{T}$ with intense ion beams or molecular cluster beams (Kim *et al.*, 1991, 1992b,c); Beuhler *et al.*, 1990; Bae *et al.*, 1991) may give higher counting rates and hence provide quantitative and conclusive tests of the revised fusion rate $R_{\text{new}}^{\text{beam}}$ due to CMEE. The recent low-energy data (Vandenbosch *et al.*, 1991) for $\text{D}(\text{D}, p)\text{T}$ fusion rates obtained with both ion and deuterated cluster beams (which do not have beam contaminant problems) on deuterated targets are lower by a factor of ~ 2 than the conventional estimates and hence may be consistent with our prediction based on $R_{\text{new}}^{\text{beam}}$, equation (5.2). A new quantitative analysis of their data is in progress. More low-energy data for the $\text{D}(\text{D}, p)\text{T}$ reaction as well as other fusion reactions with intense ion or (large-size) cluster beams and different target compositions are needed to test $R_{\text{new}}^{\text{beam}}$, equation (5.2), conclusively. We note that the CME are substantially reduced (or negligible) for (dilute) gas targets.

For the purpose of extrapolating $\sigma(E)$ to low energies from the experimental values of $\sigma_{\text{exp}}(E)$ at higher energies, we use equation (5.5) rather than equation (5.3) for convenience, since both yield similar values for $\sigma(E)$ at low energies. The proton transmission coefficient $T_{ns}(E)$, equation (5.6), is calculated with $V_0 = 46$ MeV and $R = 3.2$ fm [(1.25 fm) $A^{1/3} + 0.8$ fm (proton radius)], using equations (5.6a) and (5.6b). For comparison of the calculated values of $T_{ns}(E)$ with $T_G(E) = \exp(-E_G^{1/2}/E^{1/2})$, the ratio $T_G(E)/T_{ns}(E)$ is plotted as a function of E in Fig. 3. The calculated values of $T_{ns}(E)$ are then used to extract a new S -factor, $\tilde{S}_{\text{exp}}(E)$, from the experimental data (Filippone *et al.*, 1983; Kavanagh *et al.*, 1969) for $\sigma_{\text{exp}}(E)$, $117 \lesssim E \lesssim 1230$ keV, with the parametrization equation (5.5), i.e., $\tilde{S}_{\text{exp}}(E) = \sigma_{\text{exp}}(E)E/T_{ns}(E)$. We use the following expression for $\tilde{S}(E)$:

$$\tilde{S}(E) = \tilde{S}_{\text{NR}}(E) + \tilde{S}_{\text{R}}(E) = \left[\sum_{i=0}^n S_i E^i + \frac{G}{(E_r - E)^2 + \Gamma^2/4} \right] \quad (6.2)$$

where $\tilde{S}_{\text{NR}}(E)$ is the nonresonant contribution and $\tilde{S}_{\text{R}}(E)$ is the contribution from the resonance at $E_r \approx 630$ keV (CM). The parameters S_i , G , E_r ,

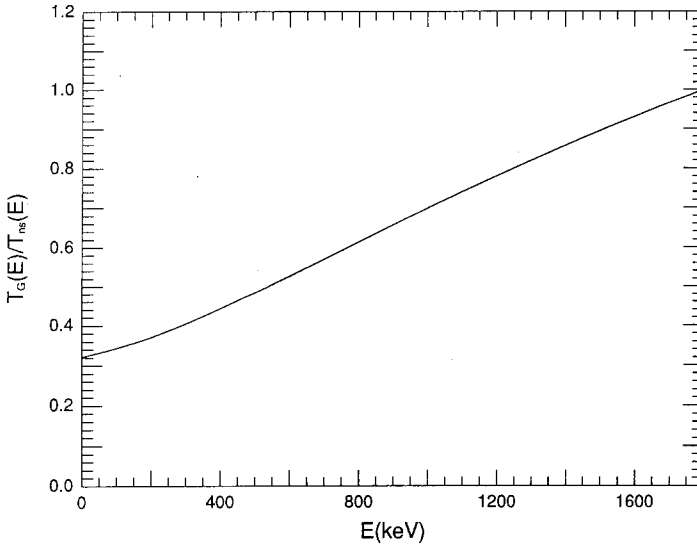


Fig. 3. Ratio of transmission coefficients $T_G(E)/T_{ns}(E)$ as a function of E . The $T_G(E)$ is calculated with $T_G(E) = \exp(-E^{1/2}/E^{1/2})$ and $T_{ns}(E)$ is calculated from equation (5.6).

and Γ are determined by fitting $\tilde{S}(E)$, equation (6.2), to $\tilde{S}_{\text{exp}}(E)$. The extracted values of the parameters for the case of $R = 3.2$ fm are $E_r = 632.4$ keV, $\Gamma = 38.16$ keV, and $G = 2.51$ keV³-b, $S_0 = 0.818 \times 10^{-3}$ keV-b, $S_1 = 0.940 \times 10^{-6}$ b, and $S_2 = 0.655 \times 10^{-9}$ keV⁻¹-b, for the $\sigma_{\text{exp}}(E)$ data of Filippone *et al.* (1983). For the $\sigma_{\text{exp}}(E)$ of Kavanagh *et al.* (1969), we obtain $E_r = 631.4$ keV, $\Gamma = 39.26$ keV, $G = 3.30$ keV³-b, $S_0 = 1.08 \times 10^{-3}$ keV-b, $S_1 = 1.30 \times 10^{-6}$ b, and $S_2 = 1.03 \times 10^{-9}$ keV⁻¹-b. These values of the parameters are used to calculate $\tilde{S}(E)$, equation (6.2), and the calculated results for $\tilde{S}(E)$ are plotted in Fig. 4.

In a similar manner, the use of equation (3.5) yields $E_r = 632.0$ keV, $\Gamma = 38.08$ keV, $G = 27.70$ keV³-b, $S_0 = 1.61 \times 10^{-2}$ keV-b, $S_1 = 3.47 \times 10^{-6}$ b, and $S_2 = 1.17 \times 10^{-9}$ keV⁻¹-b for the data of Filippone *et al.* (1983). For the data of Kavanagh *et al.* (1969), we obtain $E_r = 631.0$ keV, $\Gamma = 39.22$ keV, $G = 36.57$ keV³-b, $S_0 = 2.13 \times 10^{-2}$ keV-b, $S_1 = 5.25 \times 10^{-6}$ b, and $S_2 = 3.02 \times 10^{-9}$ keV⁻¹-b. These values of the parameters are used to calculate $S(E)$ in equation (3.5) using equation (6.2), and the calculated values of $S(E)$ are plotted in Fig. 5.

The resultant $S(E)$ and also $\tilde{S}(E)$ are used to calculate $\sigma_G(E)$ from equation (3.5), and $\sigma_{ns}(E)$ from (5.5). For comparison, the ratio $\sigma_G(E)/\sigma_{ns}(E)$ is plotted as a function of E in Fig. 6 using data of Filippone *et al.* (1983) (solid curve) and Kavanagh *et al.* (1969) (dashed curve). We

note that although $T_G(E)$ and $S_G(E)$ are very different from $T_{ns}(E)$ and $\tilde{S}(E)$, respectively, $\sigma_G(E)$ and $\sigma_{ns}(E)$ are similar within $\sim 10\%$, which indicates that both equations (3.5) and (5.5) can provide a reasonable model-independent procedure for extrapolating $\sigma_{\text{exp}}(E > 100 \text{ keV})$ to lower energies.

An important advantage of using equation (5.5) with equation (5.6) for proton tunneling is that equations (5.5) and (5.6) for the (p, γ) reaction are directly related to the (n, γ) reaction. For the (n, γ) reaction, the

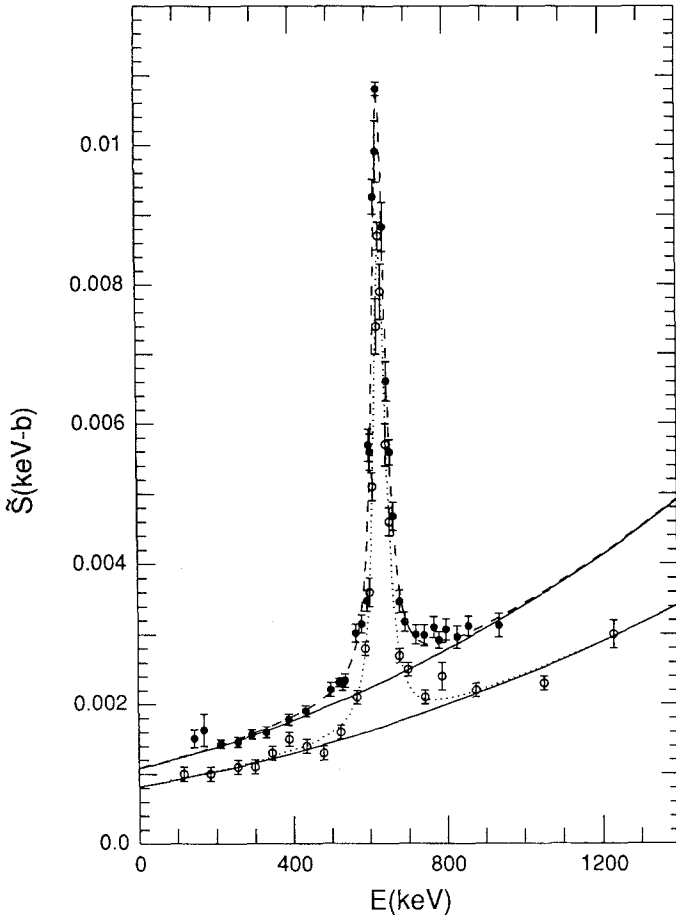


Fig. 4. S -factors calculated from equation (6.2) by fitting the experimental data (open circles) of Filippone *et al.* (1983) [lower solid curve, $\tilde{S}_{\text{NR}}(E)$; lower dotted line, $\tilde{S}_{\text{NR}}(E) + \tilde{S}_{\text{R}}(E)$] and the data (solid circles) of Kavanagh *et al.* (1969) (upper solid and dashed curves). The data of Kavanagh *et al.* (1969) for $140 < E(\text{CM}) < 3500 \text{ keV}$ are used for fitting but are not shown for $E > 1300 \text{ keV}$.

replacement of \tilde{F}_0 and \tilde{G}_0 in equations (5.6), (5.6a), and (5.6b) with the spherical Bessel functions j_0 and n_0 leads to the appropriate energy dependence for the (n, γ) cross section, $\sigma(E) \propto \tilde{S}(E)/v$, at low energies (Blatt and Weisskopf, 1952), while the use of the conventional form, equation (3.5), cannot provide the direct relationship between (p, γ) and (n, γ) reactions.

Our extrapolation method involves two parameters, $V_0 \approx 46$ MeV and r_N , but our results for $\sigma(E)$ at low energies are insensitive to V_0 , since V_0 is effectively determined and absorbed in $\tilde{S}(E)$ when $\tilde{S}(E)$ is fitted to the experimental data. Our extrapolated $\sigma(E)$ vary only by $\sim 2\%$ when r_N is

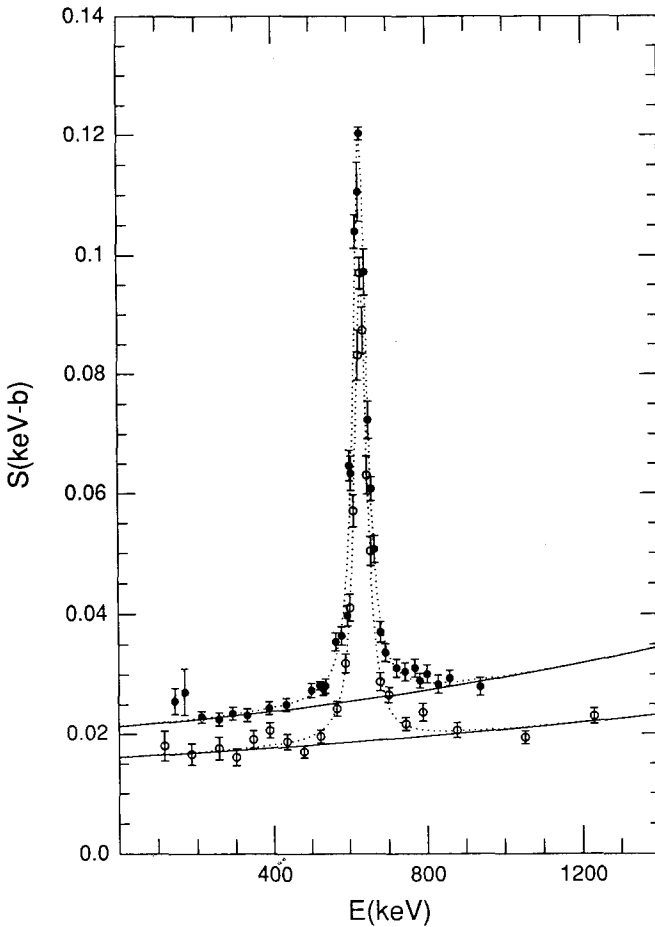


Fig. 5. Same as Fig. 4, but S -factors $S(E)$ calculated from equation (3.5).

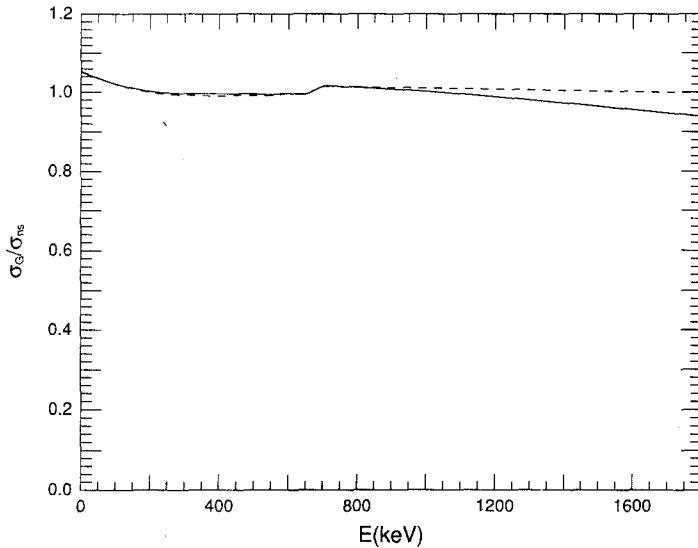


Fig. 6. Ratio of cross sections $\sigma_G(E)/\sigma_{ns}(E)$ as a function of E calculated from the experimental data of Filippone *et al.* (1983) (solid curve) and the data of Kavanagh *et al.* (1969) (dashed curve). $\sigma_G(E)$ and $\sigma_{ns}(E)$ are calculated from $S(E)$ and $\tilde{S}(E)$ using equations (3.5) and (5.5), respectively.

changed from $r_N = (1.25 \text{ fm}) A^{1/3} = 2.39 \text{ fm}$ to $r_N = 3.2 \text{ fm}$. The extracted resonance parameters, E_r , Γ , and G , in equation (6.2) are also insensitive to variations of $T_{ns}(E)$ due to the above changes in r_N . In the following, both $\sigma_G(E)$ and $\sigma_{ns}(E)$ will be used for $\langle \sigma v \rangle_{\text{conv}}$ and $\langle \sigma v \rangle_{\text{new}}$, given by equations (3.4) and (5.11), respectively, for the case of the ${}^7\text{Be}(p, \gamma){}^8\text{B}$ reaction in the sun.

6.2. Revised Fusion Rates in the Sun

For the interior core of the sun (Bahcall and Ulrich, 1988), we assume $kT \approx 1.2 \text{ keV}$, $\rho \approx 100 \text{ g/cm}^3$, and mass fractions of $X({}^1\text{H}) \approx 0.5$, $X({}^4\text{He}) \approx 0.5$, and $X({}^7\text{Be}) \approx 10^{-11}$ at a distance of ~ 0.08 solar radius from the solar center. Then $\xi = \sum_i X_i (Z_i^2 + Z_i)/A_i \approx 1.75$ and the Debye–Hückel screening radius (Salpeter, 1954) in equation (4.1) is given by $a = (kT/4\pi e^2 \rho N_A \xi)^{1/2} \approx 0.25 \text{ \AA}$.

For both ${}^7\text{Be}(p, \gamma){}^8\text{B}$ and $p(p, e^+ \nu)\text{D}$ in the sun, the assumption $r_{es} = 0$ used in equation (4.17) is justified since both $Z_i Z_j e^2 \exp[-r_s(j)/a]/r_s(j)$ and $Z_i Z_k e^2 \exp[-r_s(k)/a]/r_s(k)$ are on the order of $\sim (10\text{--}100) \text{ eV}$, while $kT \approx 1.2 \text{ keV}$. In the following, equation (4.17) will be used for both ${}^7\text{Be}(p, \gamma){}^8\text{B}$ and $p(p, e^+ \nu)\text{D}$ reactions in the sun.

6.2.1. ${}^7\text{Be}(p, \gamma){}^8\text{B}$ in the Sun

For ${}^7\text{Be}(p, \gamma){}^8\text{B}$ in the sun, we identify i, j , and k in equation (4.17) as ${}^7\text{Be}$, p , and ${}^4\text{He}$, respectively. Since $n_p = n_j = 30.11 \text{ \AA}^{-3}$ and $n_{{}^4\text{He}} = n_k = n_p/4 = 7.53 \text{ \AA}^{-3}$, the average separation distances are $n_p^{-1/3} = 0.32 \text{ \AA}$ between two protons and $(n_p + n_{{}^4\text{He}})^{-1/3} = 0.30 \text{ \AA}$ between p and ${}^4\text{He}$. Hence $r_s(j) = 0.32 \text{ \AA}$ and $r_s(k) = 0.30 \text{ \AA}$. The other numerical values are $\sigma_{kj} = 11.64$, $\delta = 1/4$, $\beta_{kj} = 2.91$, $E_s(j) = 0.180 \text{ keV}$, $E_s(k) = 0.384 \text{ keV}$ [from equation (4.10c)], $\gamma_{kj} = E_s(k)/E_s(j) = 2.13$. $F_0(E)$, equation (4.17), can be written as (E in keV)

$$F_0^{(7,1,4)}(E) = \frac{1 + 1.36E'(j)/E'(k)}{L_j^{(7)}(E) + 1.36[E'(j)/E'(k)]L_k^{(7)}(E)} \quad (6.3)$$

where $E'(j) = E + 0.180 \text{ keV}$ from equation (4.10b) and $E'(k) = E + 0.384 \text{ keV}$ from equation (4.16a). From equation (4.10a), $L_j^{(7)}(E) = 1 + [\ln(W'_{j7} + W_{j7})]/W'_{j7}W_{j7}$ with $W'_{j7} = [(E + 0.180)/0.180]^{1/2}$ and $W_{j7} = (E/0.180)^{1/2}$, and $L_k^{(7)}(E) = 1 + [\ln(W'_{k7} + W_{k7})]/W'_{k7}W_{k7}$ with $W'_{k7} = [(E + 0.384)/0.384]^{1/2}$ and $W_{k7} = (E/0.384)^{1/2}$. Numerical values of $F_0^{(7,1,4)}(E)$, equation (6.3), are plotted as a function of E in Fig. 2 (dashed curve).

Both $\sigma_G(E)$ [equation (3.5)] and $\sigma_{ns}(E)$ [equation (5.5)] with $F_0^{(7,1,4)}(E)$ calculated from equation (6.3) are used to calculate $\langle\sigma v\rangle_{\text{conv}}$ and $\langle\sigma v\rangle_{\text{new}}$, given by equations (3.4) and (5.11), respectively. The calculated results with $E_G^{1/2} = 117.48 \text{ keV}^{1/2}$ and $kT = 1.2 \text{ keV}$ for $\langle\sigma v\rangle_{\text{conv}}$ and $\langle\sigma v\rangle_{\text{new}}$ are summarized in Table I. The results in the last three

Table I. Comparison of Our New Revised Fusion Rates $\langle\sigma v\rangle_{\text{new}}$ with the Conventionally Calculated Rates $\langle\sigma v\rangle_{\text{conv}}$ for ${}^7\text{Be}(p, \gamma){}^8\text{B}^a$

| Equation used for $\sigma(E)$ [ref. for $S(E)$] | $\langle\sigma v\rangle_{\text{conv}}$ ($10^{-36} \text{ cm}^3 \text{ sec}^{-1}$) | $\langle\sigma v\rangle_{\text{new}}$ ($10^{-36} \text{ cm}^3 \text{ sec}^{-1}$) | $\langle\sigma v\rangle_{\text{new}}/\langle\sigma v\rangle_{\text{conv}}$ |
|--------------------------------------------------------|----------------------------------------------------------------------------------------|---------------------------------------------------------------------------------------|----------------------------------------------------------------------------|
| (5.5) [(a)] | 1.72 | 0.51 | 0.30 |
| (3.5) [(a)] | 1.80 | 0.54 | 0.30 |
| (5.5) [(b)] | 2.27 | 0.68 | 0.30 |
| (3.5) [(b)] | 2.38 | 0.71 | 0.30 |
| (3.5) [(c)] | 2.65 | 0.79 | 0.30 |
| (3.5) [(d)] | 2.34 | 0.70 | 0.30 |
| (3.5) [(e)] | 2.49 | 0.75 | 0.30 |

^aHere $kT = 1.2 \text{ keV}$. Data references: (a) Filippone *et al.* (1983), (b) Kavanagh *et al.* (1969), (c) Bahcall and Ulrich (1988), (d) Turck-Chièze *et al.* (1988), and (e) Bahcall and Pinsonneault (1992).

rows in Table I are obtained from equation (3.5) using $S(E) = S_0 + S_1 E$ with $(S_0, S_1) = (0.0243 \text{ keV-b}, -3 \times 10^{-5} \text{ b})$, $(0.021 \text{ keV-b}, 0.0)$, and $(0.0224 \text{ keV-b}, 0.0)$, which were used by Bahcall and Ulrich (1988), Turck-Chièze *et al.* (1988), and Bahcall and Pinsonneault (1992), respectively. As can be seen from Table I, $\langle \sigma v \rangle_{\text{new}}$ has decreased by a factor of ~ 0.30 compared with $\langle \sigma v \rangle_{\text{conv}}$.

The average total rates $R_{\nu_e}^{\text{Cl}}(\text{exp})$ of solar neutrino (electron-type, ν_e) interactions have been measured in a ^{37}Cl detector (Rowley *et al.*, 1987; Davis, 1988) via the reaction $\nu_e + ^{37}\text{Cl} \rightarrow e^- + ^{37}\text{Ar}$. The observed average values are $R_{\nu_e}^{\text{Cl}}(3.70\text{--}85) = 2.1 \pm 0.3 \text{ SNU}$ (Rowley *et al.*, 1987) and $R_{\nu_e}^{\text{Cl}}(3.70\text{--}3.88) = 2.33 \pm 0.25 \text{ SNU}$ (Davis, 1988), and $R_{\nu_e}^{\text{Cl}}(8.86\text{--}3.88) = 4.2 \pm 0.7 \text{ SNU}$ (Davis, 1988) for periods from March 1970 to the end of 1985, and from March 1970 to March 1988, and from August 1986 to March 1988 respectively, where a solar neutrino unit (SNU) is 10^{-36} interactions per target atom per second (Bahcall, 1969). Many theoretical estimates of $R_{\nu_e}^{\text{Cl}}$ based on standard solar models (SSM) (Bahcall and Ulrich, 1988; Turck-Chièze *et al.*, 1988; Bahcall and Pinsonneault, 1992) have been carried out and the latest theoretical values are $R_{\nu_e}^{\text{Cl}}(\text{total, TCCD}) = 5.8 \pm 1.3 \text{ SNU}$ (Turck-Chièze *et al.*, 1988) and $R_{\nu_e}^{\text{Cl}}(\text{total, BP}) = 8.0 \pm 3.0 \text{ SNU}$ (Bahcall and Pinsonneault, 1992). The discrepancy between the theoretical values and the experimental data is the solar neutrino problem. For the theoretical estimate $R_{\nu_e}^{\text{Cl}}(\text{total, BP})$ (Bahcall and Pinsonneault, 1992), major contributions come from five reactions: $p(p + e^-, \nu_e)\text{D}$ [$R_{\nu_e}^{\text{Cl}}(p\text{ep}) = 0.2 \text{ SNU}$], $^7\text{Be}(e^-, \nu_e)^7\text{Li}$ [$R_{\nu_e}^{\text{Cl}}(^7\text{Be}) = 1.2 \text{ SNU}$], $^7\text{Be}(p, \gamma)^8\text{Be}^*(\alpha)^4\text{He}$ [$R_{\nu_e}^{\text{Cl}}(^8\text{B}) = 6.2 \text{ SNU}$], $^{13}\text{N}(e^+ \nu_e)^{13}\text{C}$ [$R_{\nu_e}^{\text{Cl}}(^{13}\text{N}) = 0.1 \text{ SNU}$], and $^{15}\text{O}(e^+ \nu_e)^{15}\text{N}$ [$R_{\nu_e}^{\text{Cl}}(^{15}\text{O}) = 0.3 \text{ SNU}$]. If we reduce $R_{\nu_e}^{\text{Cl}}(^8\text{B}) = 6.2 \text{ SNU}$ by our CMEE reduction factor of 0.30 to $R_{\nu_e}^{\text{Cl}}(^8\text{B, CMEE}) = 1.9 \text{ SNU}$, then $R_{\nu_e}^{\text{Cl}}(\text{total, BP}) = 8.0 \text{ SNU}$ reduces to $R_{\nu_e}^{\text{Cl}}(\text{total, BP + CMEE}) = 3.7 \text{ SNU}$. In similar manner, we find that $R_{\nu_e}^{\text{Cl}}(\text{total, TCCD}) = 5.8 \pm 1.3 \text{ SNU}$ (Turck-Chièze *et al.*, 1988) reduces to $R_{\nu_e}^{\text{Cl}}(\text{total, TCCD + CMEE}) = 2.9 \text{ SNU}$, which is more consistent with the experimental values of $R_{\nu_e}^{\text{Cl}}(70.3\text{--}85) = 2.1 \pm 0.3 \text{ SNU}$ (Rowley *et al.*, 1987) and $R_{\nu_e}^{\text{Cl}}(70.3\text{--}88.3) = 2.33 \pm 0.25 \text{ SNU}$ (Davis, 1988). Most recently, a real-time, directional solar-neutrino signal has been observed in the water Cherenkov detector, Kamiokande-II (K-II) (Hirata *et al.*, 1989, 1990). The reported ratio of the neutrino flux for the period from January 1987 to April 1990 is $\phi_{\text{exp}}^{\text{K-II}}(^8\text{B}, 1.87\text{--}4.90) / \phi_{\text{SSM}}(^8\text{B, BU}) = 0.46 \pm 0.05 \text{ (stat.)} \pm 0.06 \text{ (syst.)}$ relative to the standard solar model estimate (Bahcall and Ulrich, 1988) of $\phi_{\text{SSM}}(^8\text{B, BU}) = 5.8 \times 10^6 (1 \pm 0.37) \text{ cm}^{-2} \text{ sec}^{-1}$ corresponding to $\phi_{\text{exp}}^{\text{K-II}}(^8\text{B}, 1.87\text{--}4.90) = 2.7 \times 10^6 [1 \pm 0.11 \text{ (stat.)} \pm 0.13 \text{ (syst.)}] \text{ cm}^{-2} \text{ sec}^{-1}$, which is much closer to our CMEE estimate of $\phi_{\text{CMEE}}(^8\text{B, BP}) \approx 1.74 \times 10^6 \text{ cm}^{-2} \text{ sec}^{-1}$. In a similar manner, the SSM estimate (Turck-Chièze

et al., 1988) of $\phi_{\text{SSM}}(^8\text{B, TCCD}) = 3.83 \times 10^6 \text{ cm}^{-2} \text{ sec}^{-1}$ reduces to our estimate of $\phi_{\text{CME}}(^8\text{B, TCCD}) = 1.15 \times 10^6 \text{ cm}^{-2} \text{ sec}^{-1}$.

6.2.2. $p(p, e^+ \nu) \text{D}$ in the Sun

For the reaction $p(p, e^+ \nu) \text{D}$ in the sun, indices i, j , and k in equation (4.17) are identified as p, p , and ^4He , respectively. $r_s(j) = n_p^{-1/3} = 0.32 \text{ \AA}$ for p - p pair separation and $r_s(k) = (n_p + n_{^4\text{He}})^{-1/3} = 0.30 \text{ \AA}$ for p - ^4He pair separation. $Z_k = 2$ and $Z_j = 1$ and hence $\sigma_{kj} = 6.4$. The other values are $\delta = 1/2$, $\beta_{kj} \cong 1.60$, $E_s(j) = 0.045 \text{ keV}$, $E_s(k) = 0.096 \text{ keV}$ [from equation (4.10c)], and $\gamma_{kj} = E_s(k)/E_s(j) = 2.13$. In terms of these values, equation (4.17) can be written as (E in keV)

$$F_0^{(1,1,4)}(E) = \frac{1 + 3.00E'(j)/E'(k)}{L_j^{(1)}(E) + 3.00[E'(j)/E'(k)] L_k^{(1)}(E)} \quad (6.4)$$

where $E'(j) = E + 0.045 \text{ keV}$ [from equation (4.10b)], $E'(k) = E + 0.096 \text{ keV}$ [from equation (4.10a)], $L_j^{(1)}(E) = 1 + [\ln(W'_{j1} + W_{j1})]/W'_{j1} W_{j1}$ with $W_{j1} = (E/0.045)^{1/2}$ and $W'_{j1} = [(E + 0.045)/0.045]^{1/2}$, and $L_k^{(1)}(E) = 1 + [\ln(W'_{k1} + W_{k1})]/W'_{k1} W_{k1}$ with $W_{k1} = (E/0.096)^{1/2}$ and $W'_{k1} = [(E + 0.096)/0.096]^{1/2}$. The $F_0^{(1,1,4)}(E)$ given by equation (6.4) is plotted as a function of E in Fig. 7.

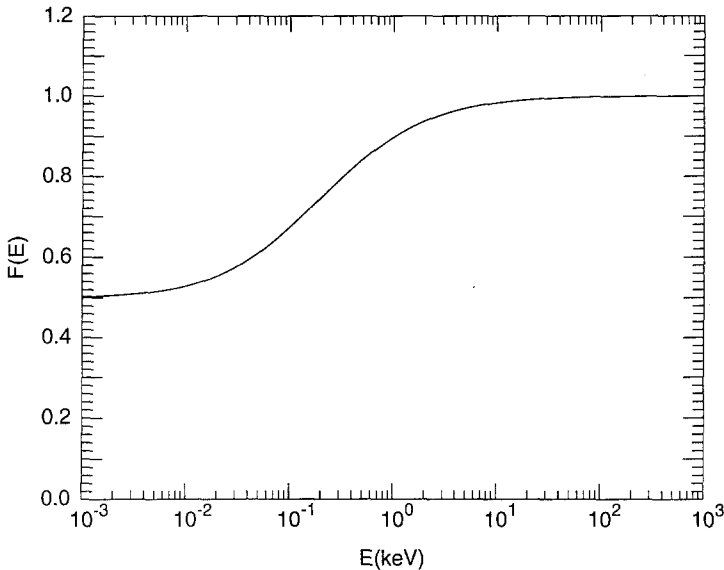


Fig. 7. Flux velocity reduction factor $F(E)$ for $p(p, e^+ \nu) \text{D}$ in the sun, equation (6.4), as a function of $E = \mu v^2/2$.

For the $p(p, e^+ \nu)D$ reaction, the fusion reaction rates are too low for determining $\sigma(E)$ in laboratory beam experiments even at higher energies (approximately several MeV). The parametric values of $S_0 = 4.07 \times 10^{-22}$ keV-b and $S_1 = 4.52 \times 10^{-24}$ b for the Maclaurin series expansion of $S(E) \approx S_0 + S_1 E$ determined from theoretically calculated $\sigma(E)$ and equation (3.5) and $F_0^{(1,1,4)}(E)$ calculated from equation (6.4) are used for SSM and solar neutrino flux calculations (Bahcall and Ulrich, 1988; Turck-Chièze *et al.*, 1988). $\sigma(E)$ calculated from equation (3.5) using the above values (Bahcall and Ulrich, 1988; Turck-Chièze *et al.*, 1988) of S_0 and S_1 , together with $E_G^{1/2} = 22.20$ keV $^{1/2}$ and $kT = 1.2$ keV, are used for our calculations of $\langle \sigma v \rangle_{\text{conv}}$ and $\langle \sigma v \rangle_{\text{new}}$, from equations (3.4) and (5.11), respectively. The calculated results are $\langle \sigma v \rangle_{\text{conv}} = 1.00 \times 10^{-43}$ cm 3 sec $^{-1}$ and $\langle \sigma v \rangle_{\text{new}} = 0.75 \times 10^{-43}$ cm 3 sec $^{-1}$, so that $\langle \sigma v \rangle_{\text{new}} / \langle \sigma v \rangle_{\text{conv}} = 0.75$, i.e., $\langle \sigma v \rangle_{\text{new}}$ is 25% smaller than $\langle \sigma v \rangle_{\text{conv}}$. *These results imply that a major revision of the conventional theory is needed.*

The recent gallium measurement (Anselmann *et al.*, 1992) of the rate of production of ${}^{71}\text{Ge}$ from ${}^{71}\text{Ga}$ by solar neutrinos yields $R_{\nu_e}^{\text{Ga}}(\text{exp}) = 83 \pm 19$ (stat.) ± 8 (syst.) SNU (1 sigma) compared with SSM prediction and 131.5_{-17}^{+21} SNU (Bahcall and Pinsonneault, 1992), of which major contributions are from reactions $p(p, e^+ \nu)D$ [$R_{\nu_e}^{\text{Ga}}(pp) = 70.8$ SNU], $p(p + e^-, \nu_e)D$ [$R_{\nu_e}^{\text{Ga}}(pep) = 3.1$ SNU], ${}^7\text{Be}(e^-, \nu){}^7\text{Li}$ [$R_{\nu_e}^{\text{Ga}}({}^7\text{Be}) = 35.8$ SNU], ${}^7\text{Be}(p, \gamma){}^8\text{B}(e^+ \nu_e){}^8\text{Be}^*(\alpha){}^4\text{He}$ [$R_{\nu_e}^{\text{Ga}}({}^8\text{B}) = 13.8$ SNU], ${}^{13}\text{N}(e^+ \nu_e){}^{13}\text{C}$ [$R_{\nu_e}^{\text{Ga}}({}^{13}\text{N}) = 3.0$], and ${}^{15}\text{O}(e^+ \nu_e){}^{15}\text{N}$ [$R_{\nu_e}^{\text{Ga}}({}^{15}\text{O}) = 4.9$ SNU]. If we reduce $R_{\nu_e}^{\text{Ga}}(pp) = 70.8$ SNU and $R_{\nu_e}^{\text{Ga}}({}^8\text{B}) = 13.8$ SNU by our CMEE reduction factors (0.75 and 0.30, respectively) to $R_{\nu_e}^{\text{Ga}}(pp, \text{CMEE}) = 53.1$ SNU and $R_{\nu_e}^{\text{Ga}}({}^8\text{B}, \text{CMEE}) = 4.14$ SNU, then $R_{\nu_e}^{\text{Ga}}(\text{total}, \text{BP}) = 131.5$ SNU (Bahcall and Pinsonneault, 1992) reduces to $R_{\nu_e}^{\text{Ga}}(\text{total}, \text{CMEE}) = 104.4$ SNU. In a similar manner, $R_{\nu_e}^{\text{Cl}}(\text{total}, \text{TCCD}) = 125 \pm$ SNU (Turck-Chièze *et al.*, 1988) reduces to $R_{\nu_e}^{\text{Cl}}(\text{total}, \text{TCCD} + \text{CMEE}) = 99.6$ SNU. These CMEE estimates are consistent with the recent result of the GALLEX experiment (Anselmann *et al.*, 1992), $R_{\nu_e}^{\text{Ga}}(\text{exp}) = 83 \pm 19$ (stat.) ± 8 (syst.) SNU (1 sigma).

7. CONDENSED MATTER INTERFERENCE (SHADOWING) EFFECT (CMIE)

We now consider another previously neglected flux reduction at high densities for nuclear fusion rates due to condensed matter interference (or shadowing) resulting from the presence of the non-fusing spectator species. This CMIE can be characterized by a set of dimensionless parameters g_j and g_k defined as $g_j = V_j n_j = 4r_j/3\lambda_j$ and $g_k = V_k n_k = 4r_k/3\lambda_k$ where V_j and V_k are the effective interaction volumes defined as $V_j = (4\pi/3)r_j^3 = [4/(3\sqrt{\pi})]\sigma_j^{3/2}$ and $V_k = (4\pi/3)r_k^3 = [4/(3\sqrt{\pi})]\sigma_k^{3/2}$. The effective interac-

tion radii r_j and r_k are for the elastic collision cross-sections, σ_j and σ_k , and are related to them as $\sigma_j = \pi r_j^2$ and $\sigma_k = \pi r_k^2$, respectively. Using equation (4.3) we obtain $\sigma_k/\sigma_j = (Z_k/Z_j)^2 (\mu_{ik}/\mu_{ij})$ and $g_k/g_j = (\sigma_k/\sigma_j)^{3/2} (n_k/n_j)$. We note that $g_k (\sim 10^3) \gg 1$, and $g_j (\sim 10^2-10^3) \gg 1$ for a dense plasma in the solar core where j is p and k is ${}^4\text{He}$.

For a low-density plasma ($g_j \ll 1$ and $g_k \ll 1$), the probability, $P_j(x)$, that i does not make an elastic collision with j in a distance x , is given by $P_j(x) = e^{-n_j \sigma_j x}$, and the number of surviving i particles at the distance x without making collisions with j is given by $I_j(x) = I(0) P_j(x) = I(0) e^{-n_j \sigma_j x}$ where $I(0)$ is the initial number of i at $x=0$. Hence, the number of i particles making collisions with j in the distance x is given by $\tilde{I}_j(x) = I(0)[1 - P_j(x)] = I(0)(1 - e^{-n_j \sigma_j x})$. The frequency f_j of the elastic collision of i with j per incident particle is then

$$f_j = \frac{1}{I_j(x)} \frac{d\tilde{I}_j(x)}{dt} = n_j \sigma_j v \quad (7.1)$$

where $v = dx/dt$ is the velocity of i . The presence of (nonfusing) k species in the low-density plasma does not affect the collision frequency f_j given by equation (7.1) significantly as long as $g_k \ll 1$, since i will encounter the same distribution of j (specified by n_j) after each elastic collision with (nonfusing) k species, if $g_k \ll 1$.

However, for a dense plasma ($g_j \gtrsim 1$ and $g_k \gtrsim 1$) such as in the solar core, the probability of continuous (sequential) multiple elastic collisions of i between two adjacent k species increases and becomes non-negligible as g_k increases. Therefore, the collision frequency f_j given by equation (7.1) is expected to be reduced to

$$\tilde{f}_j = n_j \sigma_j \tilde{v} = n_j \sigma_j v F \quad (7.2)$$

where $\tilde{v} = vF$ is the reduced effective (flux) velocity. F is the flux reduction factor given by

$$F = \frac{\tilde{f}_j}{f_j} = \frac{g_j^2 + g_j g_k}{g_j^2 + g_j g_k + g_k^2} \quad (7.3)$$

where g_j^2 , $g_j g_k$, and g_k^2 represent quantities which are proportional to the probabilities for multiple elastic collisions of i between two adjacent j species ($j \leftrightarrow i \leftrightarrow j$), between adjacent j and k species ($j \leftrightarrow i \leftrightarrow k$), and between two adjacent k species ($k \leftrightarrow i \leftrightarrow k$), respectively. We note that in the limit of $g_k \ll 1$ and $g_k \ll g_j$, $F \cong 1$, corresponding to the conventional low-density case. The new fusion rate modified by interference is given by equation (3.1) with $\langle \sigma v \rangle_{\text{conv}}$ replaced by $\langle \sigma v \rangle_{\text{new}}''$ where $\langle \sigma v \rangle_{\text{new}}'' = F \langle \sigma v \rangle_{\text{conv}}$.

For both cases of $p(p, e^+ \nu_e)D$ and ${}^7\text{Be}(p, \gamma){}^8\text{B}$ reactions in the solar core, indices j and k are identified as p and ${}^4\text{He}$, respectively, and we get $(\sigma_k/\sigma_j) = 6.4$, $(g_k/g_j) = 4.05$, and hence $F = 0.235$. The use of $F = 0.235$ for the ${}^7\text{Be}(p, \gamma){}^8\text{B}$ reaction leads to our reduced CMIE results of 3.3 SNU (instead of BP (Bahcall and Pinsonneault, 1992) result of 8.0 SNU) and 2.7 SNU (instead of TCCD (Turck-Chièze *et al.*, 1988) result of 5.8 SNU), compared with ${}^{37}\text{Cl}$ detector results of 2.1 ± 0.3 SNU (3.70–85) (Rowley *et al.*, 1987), 2.33 ± 0.25 SNU (3.70–3.88), and 4.2 ± 0.7 SNU (8.86–3.88) (Davis, 1988). Our new results calculated with CMIE are substantial improvements over the previous SSM calculations of BP, and TCCD, and are much closer to the experimental data (Rowley *et al.*, 1987; Davis, 1988).

For the neutrino flux $\phi({}^8\text{B})$ from ${}^7\text{Be}(p, \gamma){}^8\text{B}$ reaction measured by the Kamiokande detector (Hirata *et al.*, 1989, 1990), we obtain with $F = 0.235$ the calculated values of $1.34 \times 10^6 \text{ cm}^{-2} \text{ s}^{-1}$ (instead of BP result of $5.7 \times 10^6 \text{ cm}^{-2} \text{ s}^{-1}$), $0.90 \times 10^6 \text{ cm}^{-2} \text{ s}^{-1}$, (instead of TCCD result of $3.83 \times 10^6 \text{ cm}^{-2} \text{ s}^{-1}$), compared with the experimental value of $(0.46 \pm 0.05 \pm 0.06) \times (5.7 \times 10^6 \text{ cm}^{-2} \text{ s}^{-1}) = 2.7 \times 10^6 \times (1 \pm 0.11 \pm 0.13) \text{ cm}^{-2} \text{ s}^{-1}$ (Hirata *et al.*, 1989, 1990). Our new results obtained with CMIE are much closer to the experimental data (Hirata *et al.*, 1989, 1990).

For the ${}^{71}\text{Ga}$ detector result, we obtain, with $F = 0.235$ for both $p(p, e^+ \nu_e)D$ and ${}^7\text{Be}(p, \gamma){}^8\text{B}$ reactions, the calculated results of 66.7 SNU (instead of BP result of 135.1 SNU) and 62.9 SNU (instead of TCCD result of 124.0 SNU), as compared with the GALLEX data (Anselmann *et al.*, 1992) of $(83 \pm 19 \pm 8)$ SNU. Our CMIE results are in agreement with the GALLEX data (Anselmann *et al.*, 1992), and the SAGE data (Abazov *et al.*, 1991; Garvin *et al.*, 1992) of $58_{-24}^{+17} \pm 14$ (syst.) SNU.

8. SUMMARY AND CONCLUSIONS

We have investigated previously neglected condensed matter effects (CME) on nuclear fusion rates in laboratory and astrophysical environments. We have shown that CME is negligible for nuclear fusion rates at higher energies and/or in a low-density plasma, but is significant at lower energies ($E < 20$ keV) in condensed matter. These CME together with our previously proposed corrections to fusion cross sections (Kim *et al.*, 1992a, 1993) can help to solve the solar neutrino problem.

Our calculations with CME show substantially larger fusion rate reductions for ${}^7\text{Be}(p, \gamma){}^8\text{B}$ than for $p(p, e^+ \nu)D$. Our results are in good agreement with experiment, compared with conventional fusion rate estimates.

Our conclusion has profound implications in astrophysics, since previous stellar and solar (structure and evolution) model calculations have to be redone with revised nuclear fusion rates including CME. The new results are expected to be significantly different from previous results of the conventional stellar and solar model calculations. It will also change conventional estimates for the solar neutrino flux. There are also implications for magnetic and inertial confinement fusion, since decreased nuclear fusion rates due to CME will require higher values of kT than conventional estimates for achieving ignition and breakeven. Additional CME are related to reduced volume effects which have analogs in liquids and inside nuclei and which may also be operative in unexpected ways.

CME predictions of nuclear fusion rates can more easily be tested in laboratory beam experiments using intense ion beams or large-size cluster beams (in which there are no light-ion contamination problems), which can increase the low-energy incident flux substantially as demonstrated in previous heavy-water molecular cluster beam experiments for $D(D, p)T$ reaction (Beuhler *et al.*, 1990; Bae *et al.*, 1991). There exist already published $D(D, p)T$ data (Vandenbosch *et al.*, 1991) with both ion beams and small cluster beams (in which there were no light-ion contaminant problems) that may be consistent with CME. However, additional $D(D, p)T$ experiments are needed using high-flux beams and different deuterated target compositions in order to test CME on nuclear fusion rates quantitatively. Because of the profound and important implications of CME in stellar and solar fusion and in magnetic and inertial confinement fusion, it is very important to carry out such experimental tests of CME on nuclear fusion rates using high-flux ion beams on a variety of targets containing different nuclear species.

ACKNOWLEDGMENTS

This work has been supported by the Purdue Research Foundation and the Electric Power Research Institute. We wish to thank Paul Muzikar for helpful discussions.

REFERENCES

- Abazov, A. I., *et al.* (SAGE collaboration) (1991). *Physical Review Letters*, **67**, 3332.
- Anderson, H. H., and Ziegler, J. F. (1977). *Hydrogen Stopping Powers and Ranges in All Elements*, Pergamon Press.
- Anselmann, P. J., *et al.* (GALLEX collaboration) (1992). *Physics Letters B*, **285**, 376.
- Bae, Y. K., Lorentz, D. C., and Young, S. E. (1991). *Physical Review A*, **44**, 4091.
- Bahcall, J. N. (1969). *Physical Review Letters*, **23**, 251.
- Bahcall, J. N., and Pinsonneault, M. H. (1992). *Review of Modern Physics*, **64**, 885.

- Bahcall, J. N., and Ulrich, R. K. (1988). *Review of Modern Physics*, **60**, 297, and references therein.
- Beuhler, R. J., Chu, Y. Y., Friedlander, L., Friedman, L., and Kunmann, W. (1990). *Journal of Physical Chemistry*, **94**, 7765.
- Blatt, J. M., and Weisskopf, V. F. (1952). *Theoretical Nuclear Physics*, Wiley, New York.
- Bohm, D., and Aller, L. H. (1947). *Astrophysical Journal*, **105**, 131.
- Bohr, N. (1948). *Konigelige Danske Videnskabernes Selskab Matematisk-Fysiske Meddelelser*, **18**(8).
- Davis, Jr., R. (1986). In *Proceedings of the 7th Workshop on Grand Unification, ICOBAN '86*, J. Arafune, ed., World Scientific, Singapore, p. 237.
- Davis, Jr., R. (1988). In *Proceedings of the 13th International Conference on Neutrino Physics and Astrophysics, Neutrino '88*, J. Schneps *et al.*, eds., World Scientific, Singapore, p. 518.
- Filippone, B. W., Elwyn, A. J., Davids, C. N., and Koetke, D. D. (1983). *Physical Review C*, **28**, 2222.
- Fowler, W. A., Caughlan, G. R., and Zimmermann, B. A. (1967). *Annual Review of Astronomy and Astrophysics*, **5**, 525.
- Garvin, V. N., *et al.* (SAGE collaboration) (1992). XXVI International Conference on High Energy Physics, Dallas, Texas.
- Hirata, K. S., *et al.* (1989). *Physical Review Letters*, **63**, 16.
- Hirata, K. S., *et al.* (1990). *Physical Review Letters*, **65**, 1297.
- Kavanagh, R. W., Tombrello, T. A., Mosher, J. M., and Goodman, D. R. (1969). *Bulletin of American Physical Society*, **14**, 1209.
- Kennard, E. H. (1938). *Kinetic Theory of Gases*, McGraw-Hill, New York.
- Kim, Y. E., Rabinowitz, M., Bae, Y. K., Chulick, G. S., and Rice, R. A. (1991). *Modern Physics Letters B*, **5**, 941.
- Kim, Y. E., Yoon, J.-H., Rice, R. A., and Rabinowitz, M. (1992a). Solar neutrino problem with a realistic barrier solution, in *Proceedings of the 1992 Benjamin Franklin Symposium in Celebration of the Discovery of the Neutrino*, World Scientific, Singapore.
- Kim, Y. E., Yoon, J.-H., Rice, R. A., and Rabinowitz, M. (1992b). *Physical Review Letters*, **68**, 373.
- Kim, Y. E., Yoon, J.-H., Rice, R. A., and Rabinowitz, M. (1992c). *Modern Physics Letters B*, **6**, 573.
- Kim, Y. E., Rabinowitz, M., Yoon, J.-H., and Rice, R. A. (1993). *International Journal of Theoretical Physics*, **32**, 301.
- Kuo, T. K., and Pantaleone, J. (1989). *Review of Modern Physics*, **61**, 937.
- MacDonald, W. M., Rosenbluth, M. N., and Chuck, W. (1957). *Physical Review*, **107**, 350.
- Maxwell, J. C. (1866). *Philosophical Transactions CLVII* [Reprinted in *The Scientific Papers of James Clerk Maxwell*, W. D. Niven, ed., Dover, New York (1965), Vol. 2, p. 26].
- Rowley, J. K., Cleveland, B. T., and Davis, Jr., R. (1987). In *AIP Conference Proceedings*, No. 126 (1985), M. L. Cherry, K. Lande, and W. A. Fowler, eds., p. 1.
- Salpeter, E. E. (1954). *Australian Journal of Physics*, **7**, 373.
- Schiff, L. I. (1968). *Quantum Mechanics*, 3rd ed., McGraw-Hill, New York.
- Turck-Chièze, S., Cahn, S., Cassé, M., and Doom, C. (1988). *Astrophysical Journal*, **335**, 415.
- Vandenbosch, R., Trainor, T. A., Will, D. I., Neubauer, J., and Brown, I. (1991). *Physical Review Letters*, **67**, 3567.